PREPARED FOR THE U.S. DEPARTMENT OF ENERGY,
UNDER CONTRACT DE-AC02-76-CHO-3073

PPPL-3027
UC-426

PPPL-3027

A LINEAR SYSTEMS DESCRIPTION OF THE CO_2 LASER BASED TANGENTIAL IMAGING SYSTEM

BY

E. LO, J. WRIGHT AND R. NAZIKIAN

JANUARY 1995

PPPL PRINCETON PLASMA PHYSICS LABORATORY

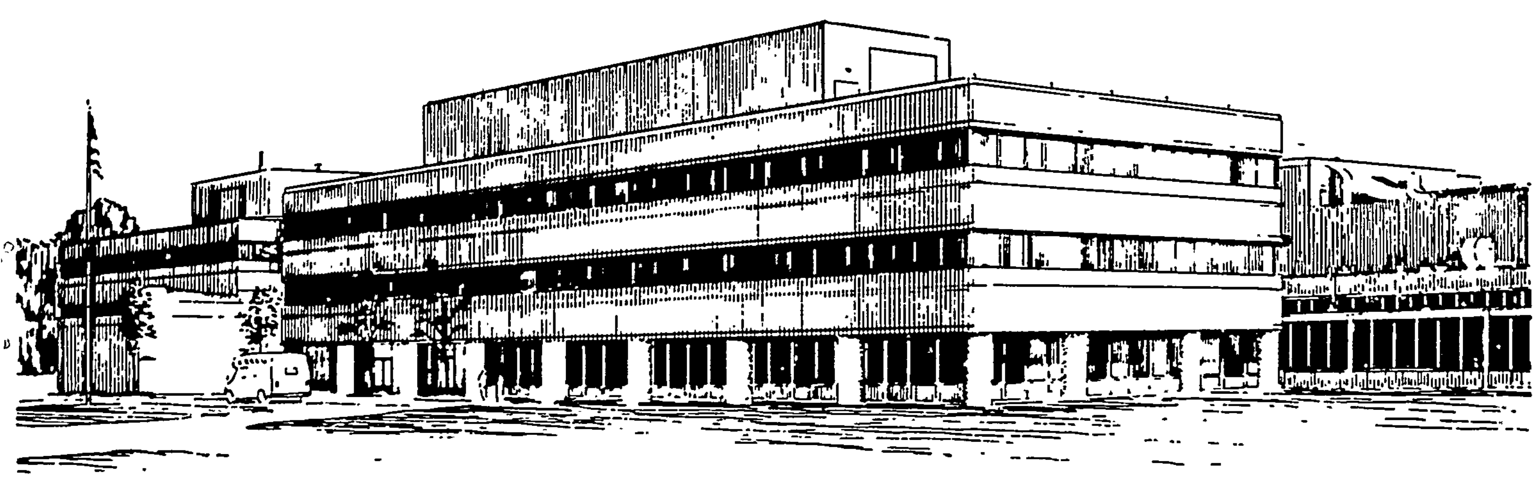

PRINCETON UNIVERSITY, PRINCETON, NEW JERSEY

NOTICE

This report has been reproduced from the best available copy.
Available in paper copy and microfiche.

Number of pages in this report: 19

DOE and DOE contractors can obtain copies of this report from:

Office of Scientific and Technical Information
P.O. Box 62
Oak Ridge, TN 37831;
(615) 576-8401.

This report is publicly available from the:

National Technical Information Service
Department of Commerce
5285 Port Royal Road
Springfield, Virginia 22161
(703) 487-4650

DISCLAIMER

Portions of this document may be illegible in electronic image products. Images are produced from the best available original document.

A Linear Systems Description of the CO_2 Laser Based Tangential Imaging System

E. Lo, J. Wright, and R. Nazikian.

Princeton Plasma Physics Laboratory, P.Ø. Box 451, Princeton University, Princeton, NJ 08543-0451

Abstract

We demonstrate that the phase variation produced by the projection of the density fluctuations onto a laser beam that is aligned tangent to the magnetic field lines in a toroidal plasma, is in fact a convolution of the density fluctuation profile in the tangency plane with a shift-invariant point spread function. Thus a spatial filter can be used to invert the corresponding transfer function to produce an undistorted image of the plasma density fluctuations at the tangency plane. Numerical simulations demonstrate that a spatial filter consisting of a simple and versatile step-function form of a Zernike phase mirror, will recover a reasonably accurate image of the fluctuations. [1]

1. Introduction

A CO_2 Laser Based Tangential Imaging System is being developed on CDX-U, which can, in principle, measure the two dimensional structure of density fluctuations in a toroidal plasma device [1]. The diagnostic overcomes two limitations of standard scattering techniques: good spatial resolution (under .5cm) is achievable for long fluctuation wavelengths; also the evolution in time of the entire spectrum of interest (.5cm - 8cm wavelengths) can be recovered from a spatially resolved image of the fluctuations [2], [3], [4].

A CO_2 laser operating at 10.6 microns is used to form an image of the plasma (electron) density fluctuations. The Gaussian laser beam is expanded to an 8cm diameter by a diverging lens, and then collimated by an off-axis parabolic mirror. The beam is then passed through the CDX-U tokamak along a horizontal chord that is aligned tangent to the magnetic field lines. The phase shifted beam is focussed by an imaging lens onto a phase mirror and then recollimated onto a horizontal detector array located at the image plane. The plane that contains the tangent points between the beam and the field lines is termed the tangency plane. Fig. 1 shows this and the geometry of the beam on CDX-U.

The technique uses the approximate uniformity of fluctuations along the magnetic field lines to recover an image of the plasma density fluctuations localized to the tangency plane [5]. As described by Nazikian and Grek [2], the effect of a projection through a toroidally symmetric plasma is to alias short wavelength features in the fluctuation profile into long wavelength, radial streaks in the projection. Since the nature of the aliasing feature is deterministic, it may be removed by focal plane filters.

In this paper we demonstrate that the projection of an object at the tangency plane through a toroidally symmetric plasma, can be represented to a good approximation by a shift-invariant point spread function acting on the object distribution. Thus a modified Zernike phase mirror must be implemented to recover the undistorted Fourier spectrum of the object. Understanding that the primary effect of the point spread function is to produce long wavelength radial streaks in the image leads to a simple and versatile step-function design for a practical phase mirror, whose action approximates the required transfer function.

2. Derivation of the Point Spread Function

We assume a toroidally symmetric plasma and also that $1/q = 0$, where q is the safety factor. The beam center at the object or tangency plane is located at $x = -R_0, y = 0, z = 0$, where x is the horizontal coordinate across the beam, y is the vertical coordinate, and z is in the direction of beam propagation.

The plasma density fluctuations are mapped onto a variation in phase on the laser beam by a line integration (i. e. , a projection) through the plasma. In the absence of diffraction effects, the phase of the wave front is given by:

$$\phi(x_1, y) = (\frac{\lambda e^2}{c^2 m_e} \frac{1}{4\pi\epsilon_o}) \int n_e(x = x_1 - R_o, y, z) dz, \quad (1)$$

where $\epsilon_0 = 8.854\text{x}10^{-12} F/m$, n_e is the plasma electron density, and the range of integration is over the plasma chord. The beam centered coordinate, $(x_1 = x + R_0)$, will be used for simplicity, from this equation on. It is assumed that R_0 is a constant over the beam cross-section.

Assuming the uniformity of fluctuations along the field lines,

$$\phi(x_1, y) \propto \int n_e(-\sqrt{(x_1 - R_0)^2 + z^2} + R_0, y) dz. \quad (2)$$

If a Taylor expansion in x_1 and z about the tangency plane is made (this is essentially a parabolic approximation to the field lines), we obtain:

$$\phi(x_1, y) \propto \int n_e(-\sqrt{(x_1 - R_0)^2 + z^2} + R_0, y) dz \approx \int n_e(x_1 - \frac{z^2}{2R_o}, y) dz. \quad (3)$$

Substituting $u = x_1 - \frac{z^2}{2R_o}$ yields

$$\phi(x_1, y) \propto \sqrt{2R_o} \int \frac{\Theta(x_1 - u)}{\sqrt{x_1 - u}} n(u, y) du, \tag{4}$$

which is now in the form of a convolution integral, with a shift invariant optical point spread function (P.S.F.) given by:

$$h(x_1, u) = h(x_1 - u) = \frac{\Theta(x_1 - u)}{\sqrt{x_1 - u}}, \tag{5}$$

with

$$\Theta(x_1 - u) = \begin{cases} 0 & \text{for } u > x_1 \\ 1 & \text{for } u < x_1. \end{cases}$$

Note that the limits of integration are extended to $\pm\infty$ with $n(x_1, y)$ set to zero outside the laser beam cross-section. The Taylor series expansion and the approximation that R_0 is a constant, hold for $x_1/R_o \ll 1$, that is, for an imaging window that is much smaller than the major radius of its location. The first approximation is expected to be valid even though the second order term (i. e. , $z^2/2R_0$), in the expansion becomes sizeable, since the primary contributions to the integral in Eq. (2) come from the regions near the tangency plane where z is small. Fig. 2 shows the projection through the plasma of a Gaussian density disturbance, calculated from a numerical evaluation of Eq. (2), compared with that calculated from the point spread function. The two curves are identical to within a reasonable accuracy. $\Delta x/R$ for this example is $\approx .33$, as compared to only $\approx .23$ for CDX-U, where the approximation is thus expected to be better. The $1/e$ width of the disturbance is about $3cm$, which signifies a Δk_x of about $.7cm^{-1}$. The essential form of the P.S.F. is also portrayed by the solid curve in Fig. 2; the streaking of an object in the tangency plane, in the x-direction is evident.

The integral expression can be rewritten in the form of a two-dimensional convolution which is more general:

$$\phi(x_1, y) \approx \sqrt{2R_o} \int\int \frac{\Theta(x_1 - u)}{\sqrt{x_1 - u}} \delta(y - v) n(u, v)\, dudv. \tag{6}$$

Note that y variations are mapped onto the laser beam phase front with no distortion. Thus the y coordinate will be dropped for simplicity.

In frequency space the transfer function is simply the Fourier transform of the P.S.F.; Fourier transforming Eq. (5) gives:

$$\mathcal{F}\{\phi(x_1)\} \propto \mathcal{F}\{h(x_1) * n(x_1)\} = \mathcal{F}\{h(x_1)\}\, \mathcal{F}\{n(x_1)\}, \tag{7}$$

where $\mathcal{F}\{...\}$ represents the Fourier transform operation in the x direction.

Therefore,

$$\tilde{\Phi}(k_x) \propto H(k_x)\tilde{n}(k_x), \tag{8}$$

where k_x is the spatial wavenumber in the x direction of the plasma at the tangency plane, $\tilde{\Phi}(k_x) \equiv \mathcal{F}\{\phi(x_1)\}$, $\tilde{n}(k_x) \equiv \mathcal{F}\{n(x_1)\}$, and the transfer function is given by

$$H(k_x) \equiv \mathcal{F}\{h(x_1)\} = \begin{cases} \sqrt{\frac{1}{2|k_x|}} e^{+i\frac{\pi}{4}} & \text{for } k_x > 0 \\ \sqrt{\frac{1}{2|k_x|}} e^{-i\frac{\pi}{4}} & \text{for } k_x < 0 \end{cases}, . \tag{9}$$

The amplitude and phase of $H(k_x)$ are shown plotted in Fig. 3. An expansion of the transfer function shows that the $k_x = 0$ component is unshifted in phase. Note that the low k_x (long wavelength) components are greatly amplified by the transfer function.

The Fourier modes of the fluctuation profile are shifted by $\pm\pi/4$ and the power spectrum of the projection is given by the simple form:

$$S_{\tilde{\Phi}(k_x)} = |\tilde{\Phi}(k_x)|^2 \propto \frac{1}{2|k_x|} S_{\tilde{n}}(k_x), \tag{10}$$

where

$$S_{\tilde{n}}(k_x) = |\tilde{n}(k_x)|^2. \tag{11}$$

3. Imaging of the Projection with a Spatial Filter

Phase contrast imaging is used to map the phase variations in the projection into a proportional intensity variation at the image plane where the detectors are located. Use of a standard phase contrast phase mirror, however, will result in a distorted image. Spectral analysis (detailed below) of a phase mirror that introduces an asymmetry between the positive and negative spatial frequencies ($\pm k_x$), shows that it is possible to both invert the transfer function inherent in the plasma projection as well as to recover an intensity image. A simple and versatile step-function design for a practical phase mirror will be presented.

For simplicity, consider the complex amplitude distribution of light of the projection, at the image plane, for a sinusoidal phase variation in x (as before, x, y are the coordinates transverse to the beam propagation direction, z. We use 'x' here to replace x_1 from Sec. 2):

$$u(x) = u_o e^{j\phi_o sin(k_x x+\theta)} \quad (12)$$

$$\approx u_o \left\{1 + j\phi_o sin(k_x x + \theta)\right\}. \quad (13)$$

The phase mirror is located at the focal plane of the imaging lens, and so will act on the angular spectrum (i. e. , the spatial Fourier transfrom) of the projection. The spatial coordinates x', y' on the mirror which is centered on the focal point, correspond to the spatial frequencies of the projection: $x' = k_x \lambda f$, and $y' = k_y \lambda f$, where λ represents the wavelength of the light, and f represents the focal distance of the imaging lens [6].

Now consider a phase mirror with its $k_x > 0$ half having an amplitude reflection coefficient $b(k_x) \cdot e^{i\beta(k_x)}$, and its $k_x \leq 0$ half having an amplitude reflection coefficient $a(k_x)$. In this paper, a, b, and β will be used to denote $a(k_x), b(k_x)$, and $\beta(k_x)$; a_o will represent $a(k_x = 0)$. The amplitude distribution becomes:

$$u(x) = u_o \left\{ a_o + \frac{\phi_o}{2} \left[b \cdot e^{i(k_x x+\theta+\beta)} - a \cdot e^{-i(k_x x+\theta)} \right] \right\}. \quad (14)$$

Thus the $+k$ and $-k$ sidebands of the sine wave variation are reflected differently. The corresponding intensity distribution is:

$$I(x) = |u(x)|^2 \approx |u_o|^2 \left\{a_o^2 + a_o \cdot \phi_o \left[b \cdot cos(k_x x + \theta + \beta) - a \cdot cos(k_x x + \theta)\right]\right\}, \tag{15}$$

where $\phi_o \ll 1$ has been assumed so that the intensity varies linearly with ϕ_o.

Now, the expression may be rewritten for a sinusoidal density variation, $n = n_o sin(k_x x + \theta)$, using Eq. (9) for the plasma transfer function:

$$\frac{I(x)}{|u_o|^2} \approx a_o^2 + a_o \cdot \frac{\kappa n_o}{\sqrt{2|k_x|}} \left[b \cdot cos(k_x x + \theta + \beta + \frac{\pi}{4}) - a \cdot cos(k_x x + \theta + \frac{\pi}{4})\right] \tag{16}$$

$$= a_o^2 + a_o \cdot \frac{\kappa n_o}{\sqrt{2|k_x|}} \left[cos(k_x x + \theta)(b \cdot cos(\beta + \frac{\pi}{4}) - \frac{a}{\sqrt{2}}) \right. \tag{17}$$

$$\left. + sin(k_x x + \theta)(-b \cdot sin(\beta + \frac{\pi}{4}) + \frac{a}{\sqrt{2}})\right],$$

where κ is a constant of proportionality. (Note that in the preceding analysis, $k_x > 0$ always, since it is the wavenumber of a sine wave spectrum; the 'negative k' components produced by the plasma scattering are denoted by $-k_x$). One condition to recover an intensity variation that is proportional to the density fluctuations at the tangency plane, is to phase shift one of the sidebands by $\beta = arccos(\frac{a}{b\sqrt{2}}) - \frac{\pi}{4}$, and to set $a \propto b \propto \sqrt{2|k|}$. A narrow strip of finite reflectance, a_o is required to reflect the main beam located at the $k = 0$ position. See Fig. 4 for a diagram of the phase mirror.

The equation for the intensity variation at the detector plane shows that an exact image of the density fluctuations is theoretically recovered:

$$\frac{I(x)}{a_o^2|u_o|^2} = 1 + \frac{\kappa n_o}{\sqrt{2} a_o} \frac{a}{\sqrt{2|k_x|}} \left(1 - \sqrt{\frac{2b^2}{a^2} - 1}\right) sin(k_x + \theta). \tag{18}$$

Hence, $I(k_x) \propto n(k_x)$, with a 'contrast enhancement factor' equal to $1 - \sqrt{\frac{2b^2}{a^2} - 1}$.

Since a phase mirror with such reflectance properties is impractically expensive to manufacture, a much simpler yet effective alternative design is considered for the experiment: the reflectivities a, b are set to constant and finite values, with β remaining at

$arccos(\frac{a}{b\sqrt{2}}) - \frac{\pi}{4}$. The reflectance of the mirror thus takes on a step-function form. By displacing the center of the phase mirror in x', both sidebands of a long wavelength variation (ie. $sin(k_x x + \theta)$ for $k_x < k_{min}$), are passed through the 'a' half so that they interfere and cancel at the image plane. One can adjust the x' displacement to select any cutoff wavelength (k_{min}) to optimize or adjust aspects of the recovered image.

The resultant intensity variation produced by the phase mirror is:

$$\frac{I(x)}{a^2|u_o|^2} = \begin{cases} 1 + \frac{\kappa n_o}{\sqrt{2|k_x|}}\frac{1}{\sqrt{2}}\left(1 - \sqrt{\frac{2b^2}{a^2} - 1}\right) sin(k_x + \theta), & \text{for } |k_x| > k_{min} \\ 0, \text{ for } |k_x| < k_{min} \end{cases} . \quad (19)$$

Thus the amplitude factor of the plasma transfer function is approximately inverted in that the plasma primarily amplifies the long wavelength components of the density fluctuation profile, whilst the phase mirror eliminates the long wavelength components altogether. Phase distortion caused by the plasma is completely removed, however. The quality of the recovered image using this simpler phase mirror design is reasonably good according to numerical simulations. Fig. 5 shows the image recovered from a density fluctuation profile of random numbers that have been convolved with a Gaussian function of width $w_{1/e} \approx 3cm$, or $\Delta k \approx .7cm^{-1}$. We conclude from the simulation results that the step- function phase mirror design in principle, adequately removes the distortion in the projection, caused by propagation through the plasma.

4. Conclusion

We establish the somewhat counter-intuitive result that a tangential imaging beam will have a phase variation that is equal to the density fluctuation profile at the tangency plane, convolved by a shift-invariant point spread function, (for an imaging window that is much smaller than the major radius). It is shown that a modified Zernike phase mirror can be used to produce a deconvolved image of the profile. A practical, step-function phase mirror design based on the knowledge that a projection through the plasma produces long wavelength radial streaks in the image, is shown to provide adequate image recovery in numerical simulations. Hence, it is demonstrated that the localized, two dimensional structure of density fluctuations can, in principle, be imaged.

5. Acknowledgment

This work was supported by U.S. Department of Energy contract No. DE-AC02-76CH03073.

Figure Captions

Figure 1: Aerial view of the imaging geometry.

Figure 2: Comparison between a numerical simulation of (solid line), and an analytic approximation to (dashed line), Eq. (2) for a Gaussian test object with a $1/e$ width of $3cm$, located at $x_1 = 0$.

Figure 3: The amplitude and phase of the plasma transfer function plotted against wavenumber (k_x).

Figure 4: Model phase mirror with three reflection zones, corresponding to $k_x < 0, k_x = 0$, and $k_x > 0$.

Figure 5: Numerical simulation of a density fluctuation profile in the tangency plane (solid line), compared with the filtered projection (dashed line), for a model phase plate with $a = a_o \ll 1$, $b = 1$, $\beta \approx +\pi/4$.

References

[1] E. Lo, R. Nazikian, J. Wright, T. Jones, E. Chao, and M. Ono, "A Laser Based Tangential Imaging System for CDX-U", Bull. of the APS, **38**, 2005 (1993) (contributed poster presented at the 1993 APS-DPP meeting).

[2] R. Nazikian and B. Grek, Rev. Sci. Instrum. **61**, 2899 (1990).

[3] H. Weisen, Rev. Sci. Instrum. **59**, 1544 (1988).

[4] S. Coda, M. Porkolab and T.N. Carlstrom, Rev. Sci. Instrum. **63**, Part II, (1992).

[5] A. J. Wootton, et. al., Phys. Fluids B **2**, 2879 (1990).

[6] J. W. Goodman, Introduction to Fourier Optics, (McGraw-Hill Book Company, New York, 1968), pp. 77-87.

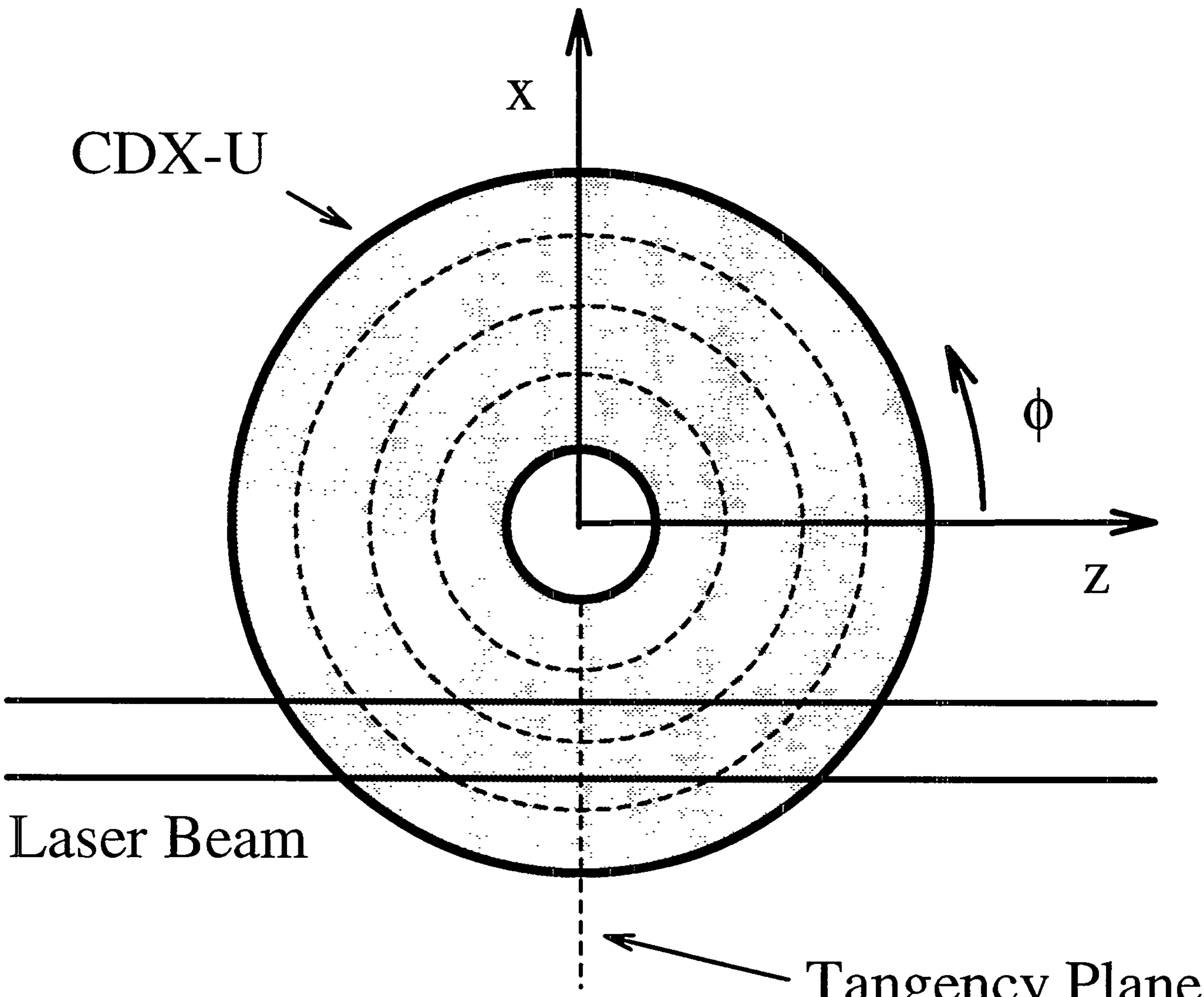

Figure 1

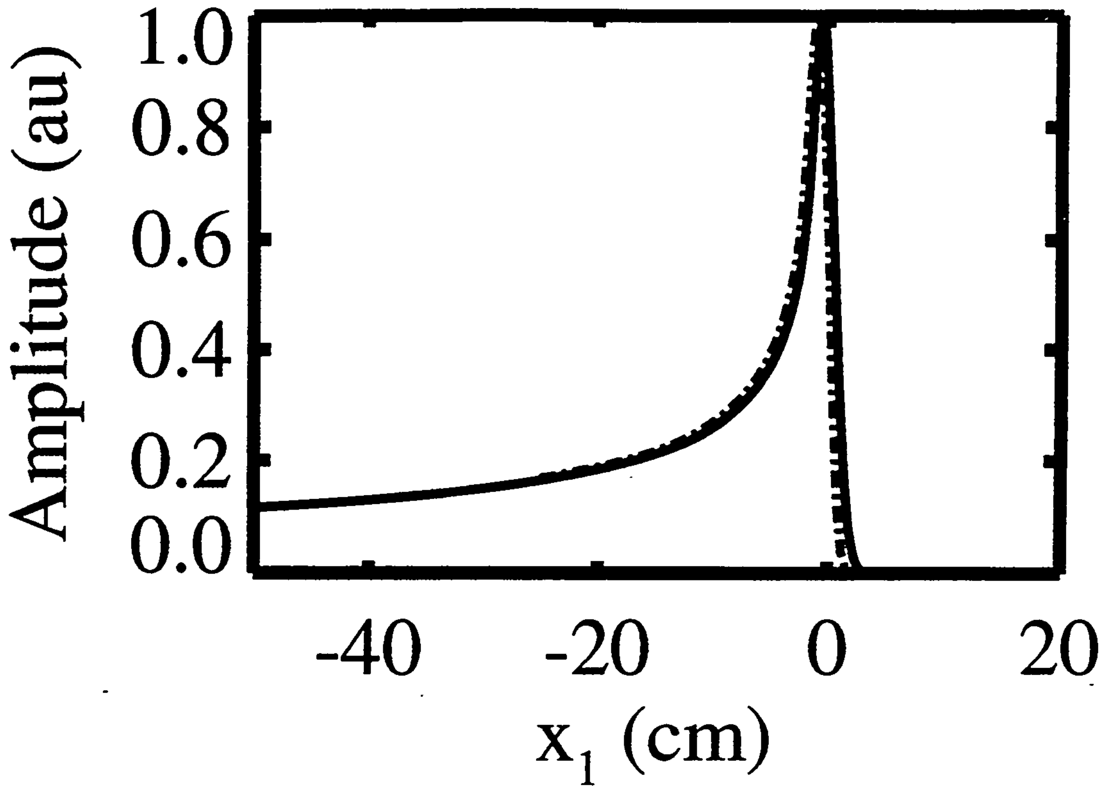

Figure 2

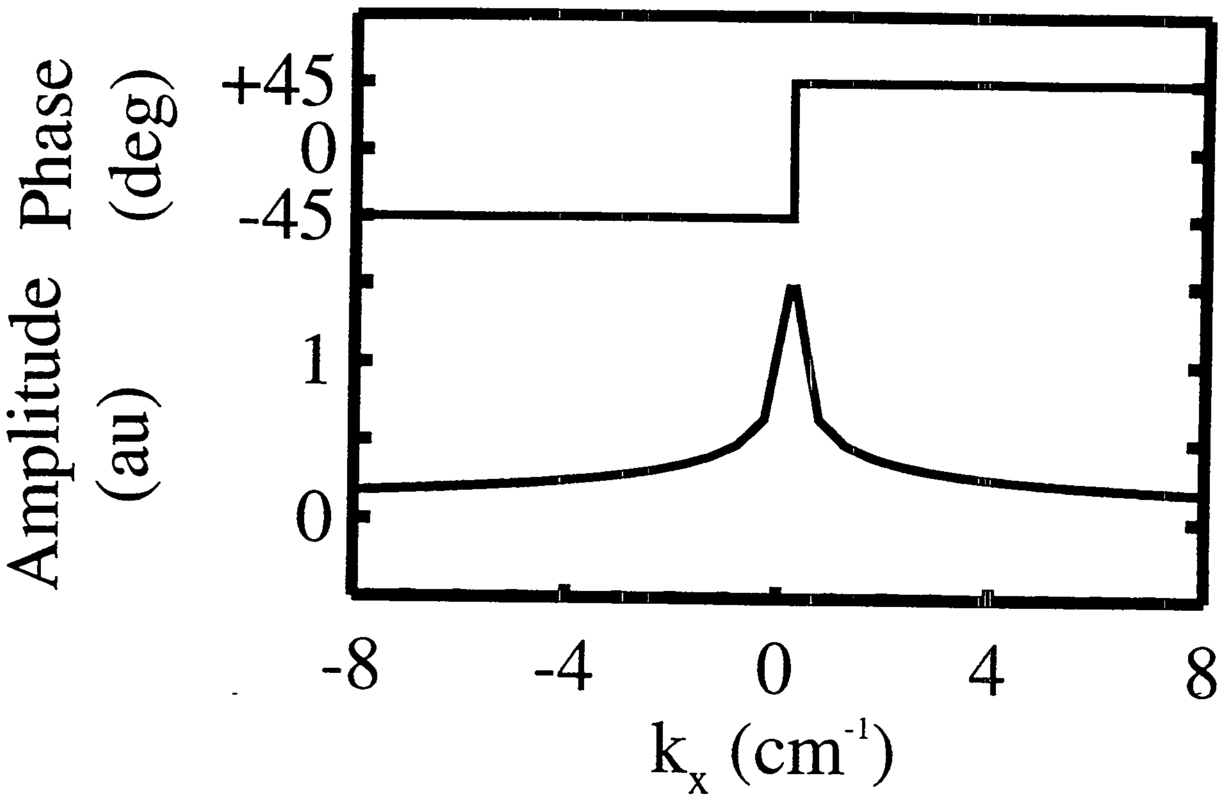

Figure 3

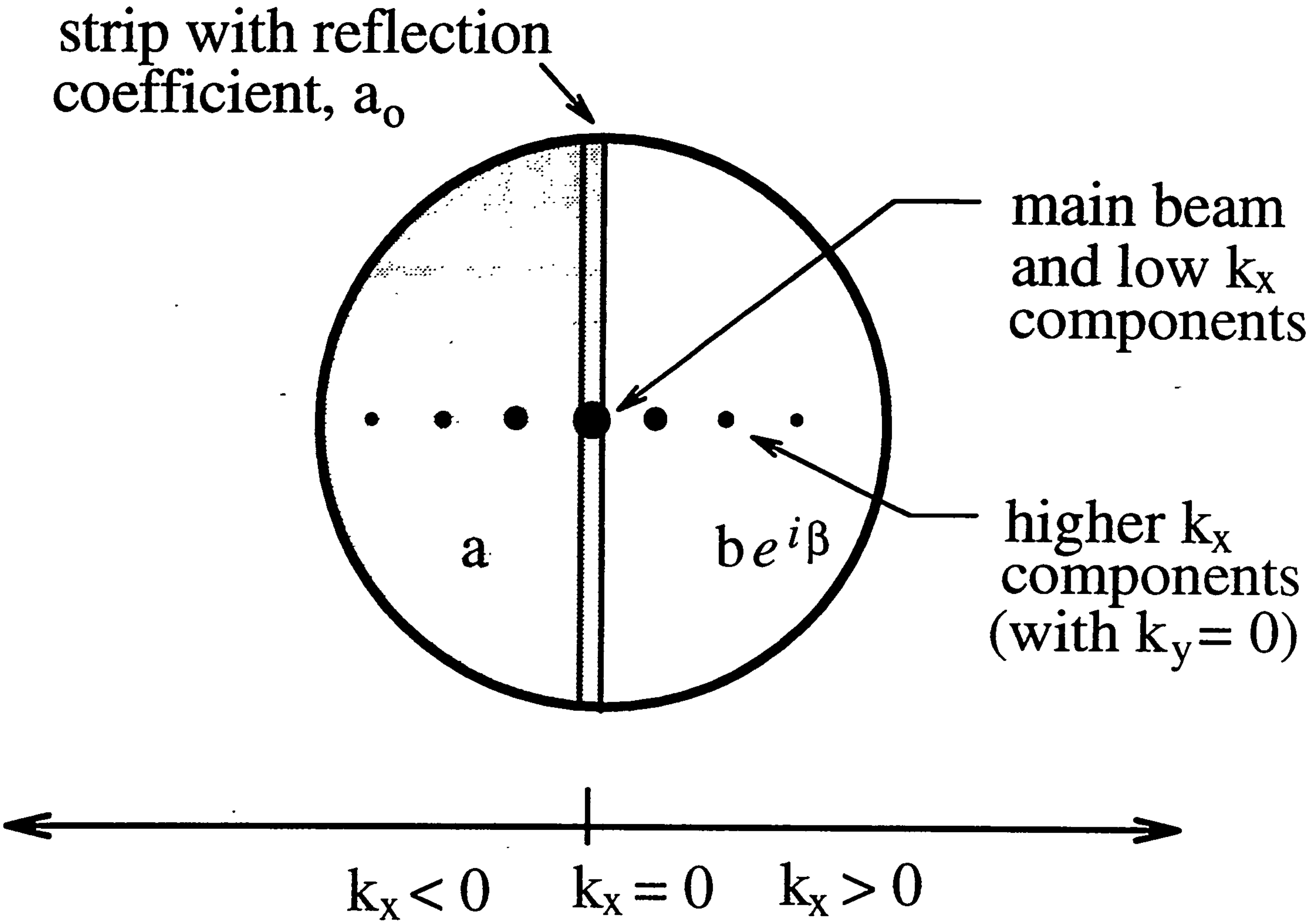
strip with reflection coefficient, a_o
main beam and low k_x components
higher k_x components (with $k_y = 0$)
a
$b e^{i\beta}$
$k_x < 0$
$k_x = 0$
$k_x > 0$

Figure 4

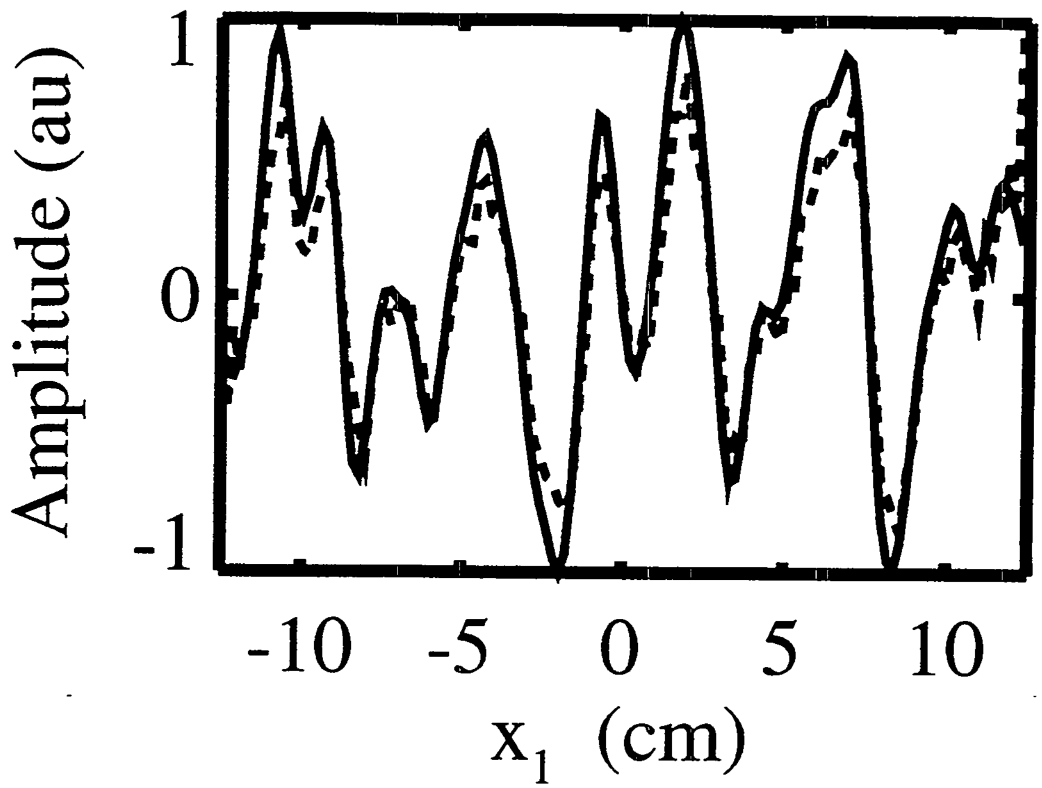

Figure 5

EXTERNAL DISTRIBUTION IN ADDITION TO UC-420

Dr. F. Paoloni, Univ. of Wollongong, AUSTRALIA
Prof. R.C. Cross, Univ. of Sydney, AUSTRALIA
Plasma Research Lab., Australian Nat. Univ., AUSTRALIA
Prof. I.R. Jones, Flinders Univ, AUSTRALIA
Prof. F. Cap, Inst. for Theoretical Physics, AUSTRIA
Prof. M. Heindler, Institut für Theoretische Physik, AUSTRIA
Prof. M. Goossens, Astronomisch Instituut, BELGIUM
Ecole Royale Militaire, Lab. de Phy. Plasmas, BELGIUM
Commission-European, DG. XII-Fusion Prog., BELGIUM
Prof. R. Boucíqué, Rijksuniversiteit Gent, BELGIUM
Dr. P.H. Sakanaka, Instituto Fisica, BRAZIL
Prof. Dr. I.C. Nascimento, Instituto Fisica, Sao Paulo, BRAZIL
Instituto Nacional De Pesquisas Espaciais-INPE, BRAZIL
Documents Office, Atomic Energy of Canada Ltd., CANADA
Ms. M. Morin, CCFM/Tokamak de Varennes, CANADA
Dr. M.P. Bachynski, MPB Technologies, Inc., CANADA
Dr. H.M. Skarsgard, Univ. of Saskatchewan, CANADA
Prof. J. Teichmann, Univ. of Montreal, CANADA
Prof. S.R. Sreenivasan, Univ. of Calgary, CANADA
Prof. T.W. Johnston, INRS-Energie, CANADA
Dr. R. Bolton, Centre canadien de fusion magnétique, CANADA
Dr. C.R. James,, Univ. of Alberta, CANADA
Dr. P. Lukác, Komenského Universzita, CZECHO-SLOVAKIA
The Librarian, Culham Laboratory, ENGLAND
Library, R61, Rutherford Appleton Laboratory, ENGLAND
Mrs. S.A. Hutchinson, JET Library, ENGLAND
Dr. S.C. Sharma, Univ. of South Pacific, FIJI ISLANDS
P. Mähönen, Univ. of Helsinki, FINLAND
Prof. M.N. Bussac, Ecole Polytechnique,, FRANCE
C. Mouttet, Lab. de Physique des Milieux Ionisés, FRANCE
J. Radet, CEN/CADARACHE - Bat 506, FRANCE
Prof. E. Economou, Univ. of Crete, GREECE
Ms. C. Rinni, Univ. of Ioannina, GREECE
Preprint Library, Hungarian Academy of Sci., HUNGARY
Dr. B. DasGupta, Saha Inst. of Nuclear Physics, INDIA
Dr. P. Kaw, Inst. for Plasma Research, INDIA
Dr. P. Rosenau, Israel Inst. of Technology, ISRAEL
Librarian, International Center for Theo Physics, ITALY
Miss C. De Palo, Associazione EURATOM-ENEA , ITALY
Dr. G. Grosso, Istituto di Fisica del Plasma, ITALY
Prof. G. Rostangni, Istituto Gas Ionizzati Del Cnr, ITALY
Dr. H. Yamato, Toshiba Res & Devel Center, JAPAN
Prof. I. Kawakami, Hiroshima Univ., JAPAN
Prof. K. Nishikawa, Hiroshima Univ., JAPAN
Librarian, Naka Fusion Research Establishment, JAERI, JAPAN
Director, Japan Atomic Energy Research Inst., JAPAN
Prof. S. Itoh, Kyushu Univ., JAPAN
Research Info. Ctr., National Instit. for Fusion Science, JAPAN
Prof. S. Tanaka, Kyoto Univ., JAPAN
Library, Kyoto Univ., JAPAN
Prof. N. Inoue, Univ. of Tokyo, JAPAN
Secretary, Plasma Section, Electrotechnical Lab., JAPAN
Dr. O. Mitarai, Kumamoto Inst. of Technology, JAPAN
Dr. G.S. Lee, Korea Basic Sci. Ctr., KOREA
J. Hyeon-Sook, Korea Atomic Energy Research Inst., KOREA
D.I. Choi, The Korea Adv. Inst. of Sci. & Tech., KOREA
Prof. B.S. Liley, Univ. of Waikato, NEW ZEALAND
Inst of Physics, Chinese Acad Sci PEOPLE'S REP. OF CHINA
Library, Inst. of Plasma Physics, PEOPLE'S REP. OF CHINA
Tsinghua Univ. Library, PEOPLE'S REPUBLIC OF CHINA
Z. Li, S.W. Inst Physics, PEOPLE'S REPUBLIC OF CHINA
Prof. J.A.C. Cabral, Instituto Superior Tecnico, PORTUGAL
Prof. M.A. Hellberg, Univ. of Natal, S. AFRICA
Prof. D.E. Kim, Pohang Inst. of Sci. & Tech., SO. KOREA
Prof. C.I.E.M.A.T, Fusion Division Library, SPAIN
Dr. L. Stenflo, Univ. of UMEA, SWEDEN
Library, Royal Inst. of Technology, SWEDEN
Prof. H. Wilhelmson, Chalmers Univ. of Tech., SWEDEN
Centre Phys. Des Plasmas, Ecole Polytech, SWITZERLAND
Bibliotheek, Inst. Voor Plasma-Fysica, THE NETHERLANDS
Asst. Prof. Dr. S. Cakir, Middle East Tech. Univ., TURKEY
Dr. V.A. Glukhikh,Sci. Res. Inst. Electrophys.I Apparatus, USSR
Dr. D.D. Ryutov, Siberian Branch of Academy of Sci., USSR
Dr. G.A. Eliseev, I.V. Kurchatov Inst., USSR
Librarian, The Ukr.SSR Academy of Sciences, USSR
Dr. L.M. Kovrizhnykh, Inst. of General Physics, USSR
Kernforschungsanlage GmbH, Zentralbibliothek, W. GERMANY
Bibliothek, Inst. Für Plasmaforschung, W. GERMANY
Prof. K. Schindler, Ruhr-Universität Bochum, W. GERMANY
Dr. F. Wagner, (ASDEX), Max-Planck-Institut, W. GERMANY
Librarian, Max-Planck-Institut, W. GERMANY